ARF1 Mediates Paxillin Recruitment to Focal Adhesions and Potentiates Rho-stimulated Stress Fiber Formation in Intact and Permeabilized Swiss 3T3 Fibroblasts

J.C. Norman,* D. Jones,‡ S.T. Barry,* M.R. Holt,* S. Cockcroft,‡ and D.R. Critchley*

*Department of Biochemistry, University of Leicester, Leicester LE1 7RH, United Kingdom; and ‡Department of Physiology, University College London, London WC1E 6JJ, United Kingdom

Abstract. Focal adhesion assembly and actin stress fiber formation were studied in serum-starved Swiss 3T3 fibroblasts permeabilized with streptolysin-O. Permeabilization in the presence of GTPγS stimulated rho-dependent formation of stress fibers, and the redistribution of vinculin and paxillin from a perinuclear location to focal adhesions. Addition of GTPγS at 8 min after permeabilization still induced paxillin recruitment to focal adhesion–like structures at the ends of stress fibers, but vinculin remained in the perinuclear region, indicating that the distributions of these two proteins are regulated by different mechanisms. Paxillin recruitment was largely rho-independent, but could be evoked using constitutively active Q71L ADP-ribosylation factor (ARF1), and blocked by NH_2-terminally truncated Δ17ARF1. Moreover, leakage of endogenous ARF from cells was coincident with loss of GTPγS-induced redistribution of paxillin to focal adhesions, and the response was recovered by addition of ARF1. The ability of ARF1 to regulate paxillin recruitment to focal adhesions was confirmed by microinjection of Q71LARF1 and Δ17ARF1 into intact cells. Interestingly, these experiments showed that V14RhoA-induced assembly of actin stress fibers was potentiated by Q71LARF1. We conclude that rho and ARF1 activate complimentary pathways that together lead to the formation of paxillin-rich focal adhesions at the ends of prominent actin stress fibers.

Key words: focal adhesions • paxillin • vinculin • rho • ARF1 • permeabilized cells

Adhesion of animal cells to the extracellular matrix is frequently mediated by members of the integrin family of cell adhesion molecules (Hynes, 1992), the cytoplasmic domains of which are linked in most, but not all cases, to cytoskeletal actin (Jockusch et al., 1995; Burridge and Chrzanowska-Wodnicka, 1996). In non-motile cells grown in culture, the components of cell–matrix junctions are localized in structures called focal adhesions. Equivalent structures are found in vivo at sites where cells exert tension on the extracellular matrix such as the myotendinous junction in skeletal muscle (Tidball, 1986) and the dense plaque in smooth muscle (Small, 1985). Focal adhesions are also found in endothelial cells subject to increased shear force (Girard and Nerem, 1995). Although there has been considerable progress in identifying and characterizing focal adhesion proteins, the complexity of the structure is such that considerable uncertainty still surrounds the role of each component (Jockusch et al., 1995). Some proteins such as talin, vinculin, and α-actinin probably provide a structural link between integrins and F-actin, whereas others such as $pp125^{FAK}$ and possibly paxillin are presumed to act in integrin-mediated signal transduction (Burridge and Chrzanowska-Wodnicka, 1996; Craig and Johnson, 1996).

In motile cells, mechanisms must exist to regulate the assembly and disassembly of cell–matrix junctions, and considerable effort has been devoted to the identification of pathways controlling these events (Burridge and Chrzanowska-Wodnicka, 1996). Studies by Hall and co-workers have shown that the Rho family of small GTP-binding proteins play a pivotal role in regulating the dynamic properties of the actin cytoskeleton (Hall, 1994; Machesky and Hall, 1996; Ridley, 1996), with Cdc42 and Rac controlling the formation of filopodia and membrane ruffling, respectively (Nobes and Hall, 1995), whilst Rho regulates the assembly of focal adhesions and actin stress fibers

S.T. Barry's current address is Receptor Systems, Glaxo-Wellcome, Medicines Research Centre, Stevenage, Herts SG1 7NY, UK.

M.R. Holt's current address is Department of Physiology, University College London, London WC1E 6JJ, UK.

Address correspondence to D.R. Critchley, Department of Biochemistry, University of Leicester, University Road, Leicester LE1 7RH, UK. Tel.: 0116-252-3477. Fax: 0116-252-5097. E-mail: drc@leicester.ac.uk

(Ridley and Hall, 1992). Much of the progress in this area has come from studies with Swiss 3T3 mouse fibroblasts that lose their focal adhesions and associated actin stress fibers when starved of serum overnight (Ridley and Hall, 1992), although adhesion remains integrin dependent (Barry et al., 1996). The addition of serum, lysophosphatidic acid (LPA),[1] or bombesin to such cells triggers the rapid assembly of focal adhesions and stress fibres in a manner which is inhibited by C3 transferase, a toxin known to ADP ribosylate and inactivate the small GTP-binding protein Rho (Ridley and Hall, 1992). Moreover, microinjection of constitutively active V14RhoA into serum-starved Swiss 3T3 cells causes the reappearance of such structures.

The effects of Rho are mediated by a number of downstream effector molecules including a Rho S/T kinase, $p160^{ROCK}$ (Leung et al., 1995; Amano et al., 1996; Matsui et al., 1996) that enhances phosphorylation of the myosin light chain and activates the actomyosin ATPase (Kimura et al., 1996). The resulting contraction of the actomyosin network is then envisaged to cause alignment of actin filaments into stress fibers, and experiments with inhibitors of the myosin ATPase have lead to the conclusion that this leads to integrin clustering and the formation of focal adhesions (Chrzanowska-Wodnicka and Burridge, 1996). Whether this pathway alone is sufficient to account for focal adhesion assembly remains to be established. In vitro, Rho has been shown to activate PI4P 5′ kinase, the enzyme that synthesizes PIP2 (Chong et al., 1994), and phospholipase D (PLD) that hydrolyzes phosphatidylcholine to phosphatidic acid (Malcolm et al., 1994; Kuribara et al., 1995; Provost et al., 1996). PIP2 is known to regulate the activity of a number of actin-binding proteins at least in vitro (Goldschmidt-Clermont, 1991; Yu et al., 1992; Fukami et al., 1996; Weekes et al., 1996; Gilmore and Burridge, 1996) and phosphatidic acid has been shown to induce actin polymerization in neutrophils (Siddiqui and English, 1997) and fibroblasts (Ha and Exton, 1993). Both pathways could contribute to the changes in the actin cytoarchitecture involved in the assembly of focal adhesions.

Cell microinjection has been crucial to many of the advances made in this field, although limitations on the number of cells that can be injected often make it impossible to analyze the cellular response at the biochemical level. However, large molecules can be introduced into cell populations permeabilized with digitonin, escin, or streptolysin-O (SL-O). For instance, Crowley and Horwitz (1995) used digitonin-permeabilized fibroblasts to study the role of actomyosin contraction and tyrosine phosphorylation in the release of cell–matrix adhesions. More recently, digitonin-permeabilized Swiss 3T3 cells were used to study events downstream of rho involved in the assembly of focal adhesions (Mackay et al., 1997). Interestingly, the ability of rho to stimulate the above responses was observed to "run-down" with time, presumably as a result of leakage or inactivation of cytosolic components after permeabilization, and addition of moesin was found to reconstitute the rhoA-stimulated assembly of actin stress fibers and vinculin-containing focal adhesions (Mackay et al., 1997). In intact cells, the formation of actin stress fibers and focal adhesions containing paxillin and vinculin is coordinately regulated (Barry and Critchley, 1994). In the present study, we have shown that (*a*) these events can be partly disconnected in SL-O permeabilized Swiss 3T3 cells and (*b*) that the small GTP-binding protein ARF1 plays a key role in the regulation of paxillin recruitment to focal adhesion–like structures.

1. *Abbreviations used in this paper:* ARF, ADP-ribosylation factor; ECM, extracellular matrix; LPA, lysophosphatidic acid; MLC, myosin light chain; PBS/ME, phosphate buffered saline/2 mM $MgCl_2$/3 mM EGTA; PLD, phospholipase D; PA, phosphatidic acid; PIP2, phosphatidyl inositol 4,5 bisphosphate; PI4P, phosphatidyl inositol 4-phosphate; SAM, substrate-attached material; SL-O, streptolysin-O.

Materials and Methods

All nucleotides were obtained from Boehringer Mannheim (Mannheim, Germany). A mouse mAb against chicken paxillin was from Transduction Laboratories (Lexington, KY) and a mouse mAb against human vinculin (F9) was a gift from V.E. Koteliansky (Laboratoire de Physiopathologie du Developpement, CNRS et Ecole Normal Superieure, Paris, France). Rat mAb anti-ARF was raised against recombinant ARF1 as described previously (Whatmore et al., 1996). Texas red– and FITC-conjugated anti–mouse immunoglobulins were from Amersham International (Little Chalfont, Buckinghamshire, UK), HRP-conjugated anti–mouse immunoglobulin was from the Sigma Chemical Co. (Poole, Dorset, UK), and rhodamine-labeled dextran was from Molecular Probes Europe BV (Leiden, The Netherlands). Enhanced chemiluminescence reagents and a Coomassie blue protein assay kit were from Pierce and Warriner Ltd. (Chester, Cheshire, UK). All other reagents including SL-O (S-5265) were purchased from Sigma Chemical Co.

Permeabilization of Swiss 3T3 Cells with Streptolysin-O

Mouse Swiss 3T3 fibroblasts were cultured in DME (GIBCO BRL, Paisley, Scotland) supplemented with 10% FCS. Cells were plated on 22 × 22-mm glass coverslips in 8-well multidishes and grown to 70–90% confluence over 3 d. Cells were then washed three times with PBS, and incubated for 20–22 h in serum-free DME. Serum-starved cells were cooled rapidly to 4°C by addition of ice-cold buffer containing 137 mM sodium glutamate, 2 mM $MgCl_2$, 1 mg/ml BSA in 20 mM Pipes, pH 6.8, and then the cells were exposed to SL-O at 100 IU/ml in buffer containing 3 mM EGTA for 10 min at 4°C. At this temperature, SL-O binds to the plasma membrane without affecting permeabilization. Excess SL-O was removed by washing with buffer, and permeabilization induced by addition of buffer at 37°C, with the free calcium concentration buffered between 50 and 100 nM using an EGTA/Ca buffer (Tatham and Gomperts, 1990). For experiments in which the cells were challenged at the time of permeabilization, 1 mM Mg ATP with or without 50 μM GTPγS was included at this point. However, in experiments that incorporated a delay between permeabilization and stimulation, the cells were permeabilized with buffer containing 1 mM GDP for various times, and then stimulated in the presence of 1 mM Mg ATP for an additional 8 min at 37°C. Cells were either fixed (10 min) in 3.8% formaldehyde in PBS containing 3 mM $MgCl_2$ and 3 mM EGTA (PBS/ME) for analysis by immunofluorescence, or transferred to ice-cold wet-cleavage buffer for analysis of substrate-attached material (SAM). Over 95% of cells were permeabilized within 2 min of raising the temperature to 37°C as judged by uptake of the membrane-impermeant dye ethidium bromide.

Microinjection of Cells

Serum-starved Swiss 3T3 cells were microinjected with either Q71LARF1, V14rhoA (both at needle concentrations of 500 μg/ml), or Δ17ARF1 (at needle concentrations of 900 μg/ml) in 50 mM Tris, pH 7.5, containing 100 mM NaCl and 1 mM $MgCl_2$ and 200 μg/ml of lysine-fixable, rhodamine-conjugated dextran MW 3000 (D-3308; Molecular Probes) to aid identification of microinjected cells. Cells were then returned to the incubator for the indicated times before either fixation or LPA stimulation followed by fixation. All injections were carried out with the aid of a Leitz micromanipulator connected to a Narishige microinjector unit.

Recombinant V14RhoA, C3-transferase, and ARF1

V14RhoA and C3-transferase were expressed in *Escherichia coli* as glu-

tathione-S-transferase fusion proteins and purified as described previously (Ridley and Hall, 1992). Protein concentrations were determined using a Coomassie blue protein assay kit with BSA as standard. V14RhoA with GTP bound was prepared by incubating the protein (1 mg/ml) with 0.5 mM GTP in 50 mM Tris, pH 7.0, containing 20 mM EDTA for 20 min, followed by the addition of 30 mM $MgCl_2$ (Hall and Self, 1986). ARF1, the constitutively active ARF1 mutant Q71LARF1, and the NH_2-terminally truncated Δ17ARF1 mutant were expressed in *E. coli* and purified as described previously (Cockcroft et al., 1994).

Cell Staining and Microscopy Techniques

For double-label confocal microscopy, fixed cells were extracted with 0.2% Triton X-100 in PBS/ME for 1 min, and non-specific protein binding sites were blocked by overnight incubation with 10% FCS in PBS/ME at 4°C. Cells were incubated with the primary mouse mAb in PBS/ME containing 0.2% BSA for 30 min at 37°C, and then after extensive washing, a Texas red–conjugated anti–mouse secondary antibody added in the same buffer. Unbound antibody was removed by extensive washing. Dilutions of the primary antibodies used were: anti-paxillin 1:400 from commercial stock, and anti-vinculin 1:25 from hybridoma supernatant. Actin filaments were visualized by incubation with 0.5 μM FITC-labeled phalloidin for 20 min at room temperature. Cells were mounted in 80% glycerol in PBS and viewed on a Leica confocal laser scanning microscope attached to a Leitz Fluorovert-FU microscope. For the detection of FITC, exitation was at 488 nm and emission was collected with a 540-nm band-pass filter (transmitting between 525 and 555 nm). For the detection of Texas red, excitation was at 514 nm and emission was collected with a >600-nm barrier filter. A stack of optical slices that encompassed the depth of the cell was obtained (normally 10 slices, 0.5 μm apart), and FITC-phalloidin fluorescence from this stack was combined using the Leica "topographic" function. This gives an extended focus image representing the actin cytoskeleton in all parts of the cell. For presentation of the Texas red fluorescence (paxillin and vinculin), the plane of adhesion was imaged as a z-optical section 0.5 μm above the coverslip, the surface of the glass being located by reflection imaging. The nuclear plane of the same field of view was then imaged at a z-optical section 3.0 μm above this. The nucleus usually, but not always, lies on this plane.

For quantitative confocal microscopy, fixed cells were incubated with mouse anti-paxillin and anti-vinculin as for double-label confocal microscopy, but the antigen was visualized using FITC-conjugated anti–mouse secondary antibody. Double staining of actin filaments with phalloidin was not performed, as small amounts of "bleed-though" fluorescence were found to interfere with quantitative analysis. Cells were viewed on a Bio-Rad MRC-500 confocal microscope using the high sensitivity blue exitation filter set (BHS). The planes of adhesion and the nucleus were located as described above, and the fluorescence intensity of each plane expressed as a percentage of the total cellular fluorescence of the same field. Total cellular fluorescence was obtained by summation of ~5 optical sections each 1 μm apart, encompassing the z-axis of the cell.

Paxillin and actin staining in microinjected cells was viewed by epifluorescence microscopy. After microinjection and fixation, actin filaments were stained with FITC-phalloidin or paxillin visualized using mouse anti-paxillin followed by FITC-conjugated anti–mouse secondary antibody. Microinjected cells were inspected using a Zeiss Axiophot microscope and photographed with Ilford HP5-400 ASA film upgraded to 1600 ASA during development.

Preparation of Substrate-attached Material by Wet Cleavage

This was performed according to the method of Brands and Feltkamp (1988). Briefly, cells were cooled immediately to 4°C by addition of ice-cold wet-cleavage buffer (25 mM Tris-HCl, pH 7.2, 135 mM NaCl, 5 mM KCl, 0.5 mM NaH_2PO_4, 1.0 mM $CaCl_2$, 5 mM $MgCl_2$). Coverslips were then placed, cell side down, onto nitrocellulose sheets (which had been pre-rinsed with wet-cleavage buffer and air dried for 10 min) for 10 min on ice. The cell bodies were removed by lifting the coverslips, and the SAM remained on the coverslip. Coverslips were then extensively washed with eight changes of wet cleavage buffer, and SAM dissolved in SDS-PAGE sample buffer for analysis by Western blotting.

Western Blotting

Proteins from cell lysates were resolved in SDS–polyacrylamide gels and electroblotted to nitrocellulose membranes for 1 h at 0.6 mA/cm^2 using a Bio-Rad semi-dry transfer cell. Excess protein binding sites were blocked by incubating (45 min) membranes in 4% lowfat milk in TBS (20 mM Tris-HCl, pH 7.5, 137 mM NaCl) containing 0.3% Tween-20. Membranes were then incubated with anti-paxillin (diluted 1:5,000) or anti-vinculin (diluted 1:400) antibodies or rat anti-ARF mAb (diluted 1:750) in TBS, 0.1% Tween-20 with 1% BSA overnight at 4°C, and bound antibody was detected with HRP-conjugated goat anti–mouse or anti–rat and enhanced chemiluminescence. Quantitation of blots was obtained by volume integration using a Molecular Dynamics scanning laser densitometer.

Results

Serum-starved Swiss 3T3 Cells Permeabilized with SL-O Assemble Focal Adhesion–like Structures Containing Vinculin and Paxillin in Response to GTPγS

Serum-starved Swiss 3T3 cells lack focal adhesions and associated actin stress fibers, and treatment of these cells with serum, LPA or bombesin (Ridley and Hall, 1992), or RGD peptides (Barry et al., 1996) stimulates the appearance of such structures, a process that is regulated, at least in part, by the small GTP-binding protein RhoA. To further investigate the biochemical mechanisms underlying these events, we explore the effects of other potential regulatory molecules using serum-starved Swiss 3T3 cells permeabilized with SL-O. This was achieved by first binding the SL-O to cells at 4°C, followed by permeabilization at 37°C. Much of the F-actin in serum-starved Swiss 3T3 cells treated in this way was localized under the plasma membrane, and as a fine meshwork throughout the body of the cell, with only occasional actin stress fibers (Fig. 1, *A* and *G*). Immunofluorescence localization of the focal adhesion proteins paxillin (Fig. 1, *B* and *C*) and vinculin (Fig. 1, *H* and *I*) by confocal microscopy revealed that these proteins were largely concentrated in the perinuclear region, with rather little staining in the plane of adhesion. When permeabilzation (shift to 37°C) was accompanied by the immediate addition of GTPγS, the cells assembled numerous actin stress fibers (Fig. 1, *D* and *J*) terminating at the cell margins in paxillin (Fig. 1 *F*) and vinculin-containing (Fig. 1 *L*) focal adhesion–like structures. There was a corresponding reduction in paxillin (Fig. 1 *E*) and vinculin staining (Fig. 1 *K*) in the perinuclear region. Quantitative analysis of the results showed that ~25% of SL-O permeabilized serum-starved cells contained actin stress fibers, and this figure increased to ~65% when cells were treated for 8 min with GTPγS (Fig. 2 *A*). Paxillin staining in the plane of adhesion increased about sevenfold and vinculin about fivefold in response to GTPγS (Fig. 2 *B*).

To determine how long SL-O–treated cells retain the capacity to respond in this way, GTPγS was added at various times after permeabilization. Addition of GTPγS stimulated actin stress fiber formation even when added 16 min after permeabilization (Fig. 2 *C*). However, the GTPγS-stimulated recruitment of paxillin to focal adhesion–like structures showed an initial rapid decay, although a significant response was retained when the GTPγS was added up to 8 min after the shift to 37°C (Fig. 2 *D*). In contrast, the GTPγS-stimulated recruitment of vinculin into focal adhesion–like structures was lost within 2 min (Fig. 2 *D*). These results suggest that the mechanisms that normally coordinate the recruitment of vinculin and paxillin to the ends of

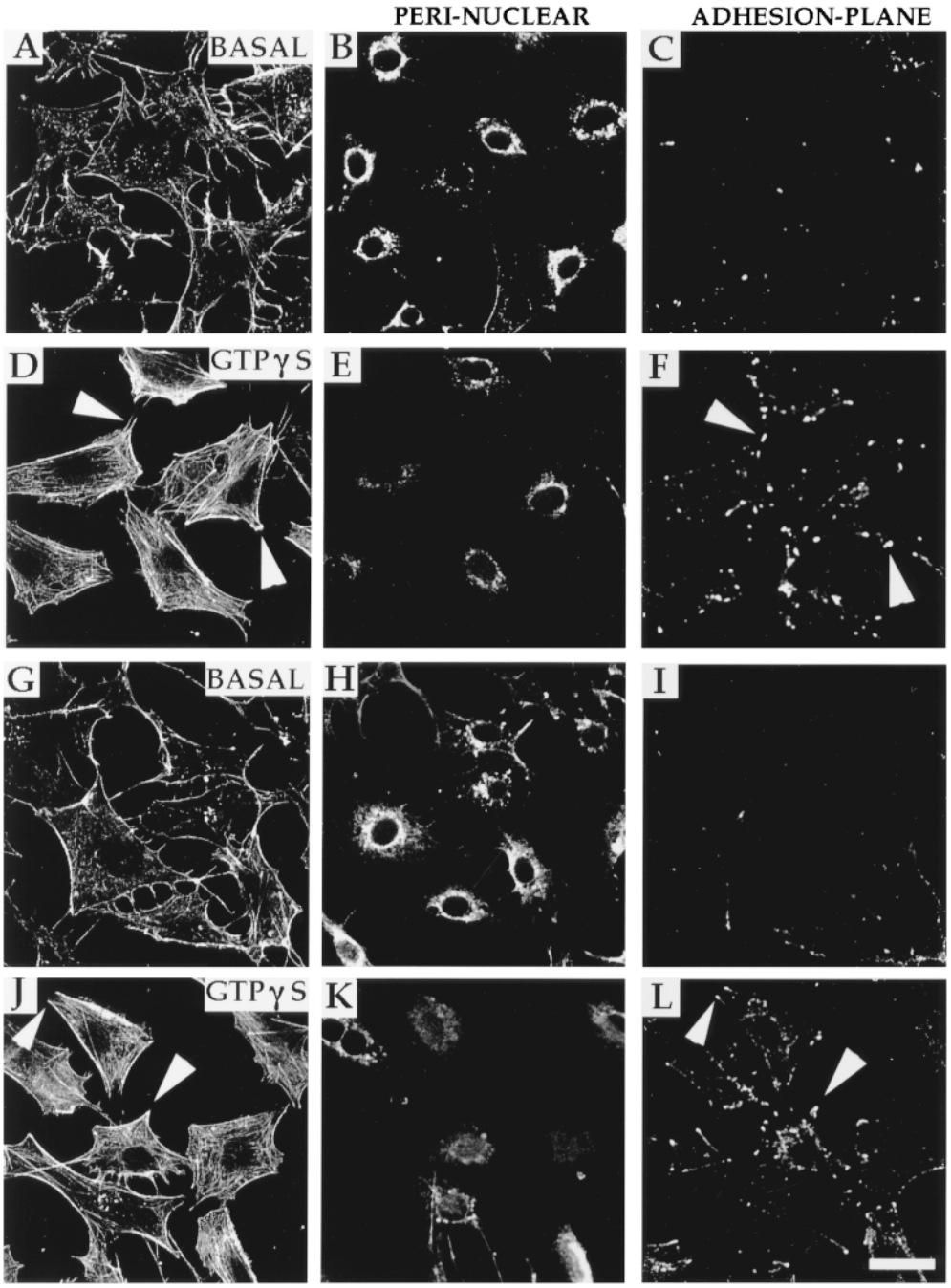

Figure 1. Addition of GTPγS to SL-O–permeabilized Swiss 3T3 cells induces the formation of actin stress fibers and focal adhesion–like structures containing paxillin and vinculin. Serum-starved Swiss 3T3 cells were incubated with SL-O on ice for 10 min, and permeabilized for 8 min in the presence of 1 mM Mg ATP in the absence (*A–C* and *G–I*; *BASAL*) or presence of 50 μM GTPγS (*D–F* and *J–L*). Cells were double stained for F-actin (*A*, *D*, *G*, and *J*), and for paxillin (*B*, *C*, *E*, and *F*) or vinculin (*H*, *I*, *K*, and *L*), and analyzed by confocal microscopy. Images from two planes of focus are presented, one centered 0.5 μm above the surface of the coverslip (*ADHESION-PLANE*) (*C*, *F*, *I*, and *L*), and another 3.0 μm above this that is across the center of the nucleus in the majority of cells (*PERI-NUCLEAR*) (*B*, *E*, *H*, and *K*). Arrowheads are in equivalent positions in the image pairs. Bar, 40 μm.

actin stress fibers become uncoupled in permeabilized cells, providing an opportunity to dissect the pathways that regulate each event. Subsequent experiments were therefore carried out using an 8-min permeabilization period, conditions under which GTPγS can stimulate the recruitment of paxillin, but not vinculin, to the ends of actin stress fibers.

GTPγS-stimulated Recruitment of Paxillin into Focal Adhesion–like Structures Is rho-independent

The ability of GTPγS to stimulate the redistribution of paxillin into focal adhesion–like structures at the ends of actin filaments (Fig. 3, *C* and *D*), could not be mimicked completely by V14RhoA. Whereas V14RhoA stimulated the appearance of numerous actin stress fibers, the recruitment of paxillin to the ends of these structures (Fig. 3 *F*) was much less pronounced than with GTPγS (Fig. 3 *D*), and much of the paxillin remained in the perinuclear region (data not shown). To establish whether the GTPγS-induced redistribution of paxillin was indeed independent of Rho, permeabilized cells were pre-treated with C3 transferase. Such treatment completely blocked the formation of actin stress fibers (Fig. 3 *G*), but failed to block the GTPγS-induced redistribution of paxillin into the plane of adhesion (Fig. 3 *H*). Under these conditions, pax-

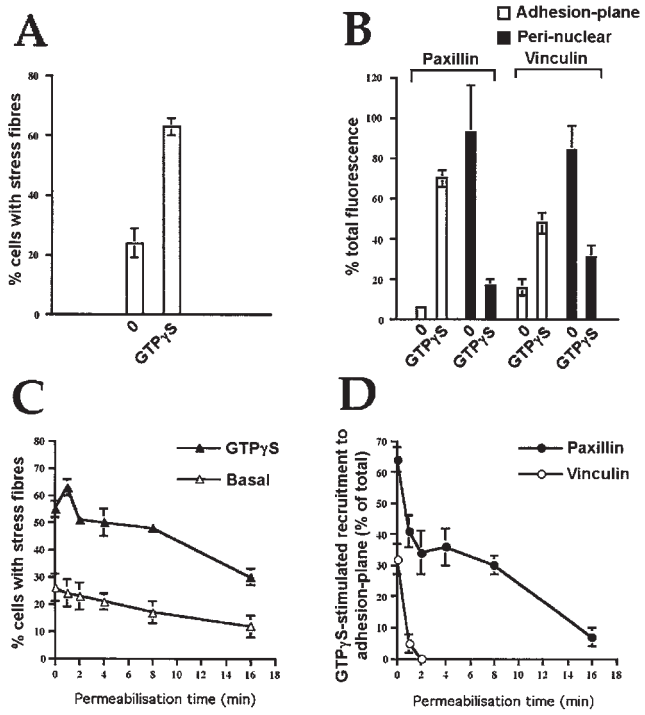

Figure 2. Quantitative analysis of the distribution of F-actin, paxillin, and vinculin staining in SL-O–permeabilized cells treated with GTPγS. (*A*) Serum-starved Swiss 3T3 cells were incubated with SL-O on ice for 10 min and permeabilized at 37°C for 8 min in the presence of 1 mM Mg ATP in the absence (*0*) or presence of 50 μM GTPγS. F-actin was visualized with FITC-phalloidin, and cells were scored for the presence of actin stress fibers. Values represent the mean (± SEM) obtained from four separate experiments. (*B*) Cells were permeabilized and stimulated with GTPγS as for *A*, and the intensities of vinculin and paxillin immunostaining within an optical plane centered 0.5 μm (adhesion-plane, *open bars*) and 3.0 μm above the surface of the coverslip (perinuclear; *closed bars*) were determined for 20 random fields. These values were expressed as a percentage of the total immunostaining from the same field determined by summation of fluorescence intensities from optical sections encompassing the depth of the cell. The data represent the mean (± SEM) of values obtained from three separate experiments. (*C*) Cells were incubated with SL-O on ice for 10 min and permeabilized by incubation at 37°C in the presence of 1 mM GDP, for various times. After this, 1 mM Mg ATP was added in the absence (△) or presence of 50 mM GTPγS (▲) for 8 min. F-actin was visualized with FITC-phalloidin, and cells were scored for the presence of actin stress fibers. Values represent the mean (± SEM) obtained from three separate experiments. (*D*) Cells were treated as in *C* and the percentage of total cellular vinculin (○) and paxillin (●) found in the plane of adhesion was determined as for *B*. The basal values (ATP alone) were then subtracted from those found in the presence of GTPγS (ATP + GTPγS), and plotted as GTPγS-stimulated recruitment of paxillin or vinculin into the plane of adhesion. These data represent the mean (± SEM) of values obtained from three separate experiments.

illin was localized in focal adhesion–like structures associated with the ends of actin filaments under the plasma membrane (Fig. 3, *G* and *H*).

Quantitative analysis of the confocal images showed that both GTPγS and V14RhoA stimulated actin stress fiber formation to about the same extent, and that the GTPγS response was completely blocked by pre-incubating the cells with C3 transferase (Fig. 3 *I*). GTPγS produced a 6.8-fold increase in paxillin fluorescence in the plane of adhesion, whereas V14RhoA produced a much smaller effect (twofold increase approximately) (Fig. 3 *J*). Furthermore, the effect of GTPγS was only partially inhibited by pre-treating cells with C3 transferase. Overall, these results suggest that Rho is not essential for the GTPγS-dependent redistribution of paxillin into focal adhesion–like structures.

Analysis of the Paxillin Content of SAM by Western Blotting

To test the hypothesis that the targeting of paxillin to focal adhesions can occur by mechanisms that are independent of Rho, focal adhesions and SAM were isolated using the technique of wet cleavage. The body of the cell is removed by overlaying the cell monolayer with a sheet of nitrocellulose, which is then peeled off, leaving behind material that is firmly attached to the extracellular matrix. The paxillin content of SAM isolated from SL-O–permeabilized, serum-starved cells (as determined by Western blotting) was low, and the addition of GTPγS 8 min after permeabilization caused a large increase in the amount of paxillin associated with SAM (Fig. 4 *A*). The run-down of the response is shown in Fig. 4 *B*. There was an initial rapid run-down in response, but GTPγS continued to cause a marked increase in the paxillin content of SAM when added up to 8 min after permeabilization. In contrast, the GTPγS-stimulated recruitment of vinculin into SAM was lost within 4 min of permeabilization. The "run-down" kinetics are very similar to those observed for the GTPγS-induced recruitment of paxillin and vinculin into focal adhesion–like structures observed using confocal microscopy (Fig. 2 *D*), and subsequent experiments were carried out 8 min after permeabilization.

Whereas GTPγS caused a marked increase in the paxillin content of SAM, V14RhoA failed to increase levels over basal values. Pre-treatment of cells with C3-transferase reduced the amount of paxillin in SAM to below the basal value, but did not block the increase seen in response to GTPγS (Fig. 4 *A*). Quantitative analysis of 4 independent experiments showed that GTPγS produced a 4.4-fold increase in paxillin in SAM, and the effect was not dependent on Rho as it was not blocked by C3 transferase (Fig. 4 *C*). However, V14RhoA produced a small (1.7-fold) increase in substrate-associated paxillin, although the effect was somewhat more variable than that produced by GTPγS as indicated by the larger standard errors. The results of the biochemical analysis of wet-cleavage material are consistent with those obtained by immunofluorescence, and confirm that the GTPγS-induced redistribution of paxillin into SAM is not Rho dependent, although Rho does have some capacity to stimulate the redistribution of paxillin into SAM.

Q71LARF1 Drives the Redistribution of Paxillin into Focal Adhesion–like Structures

Recent evidence indicates that, in mouse, the "cytoplasmic" pool of the α and β isoforms of paxillin are localized

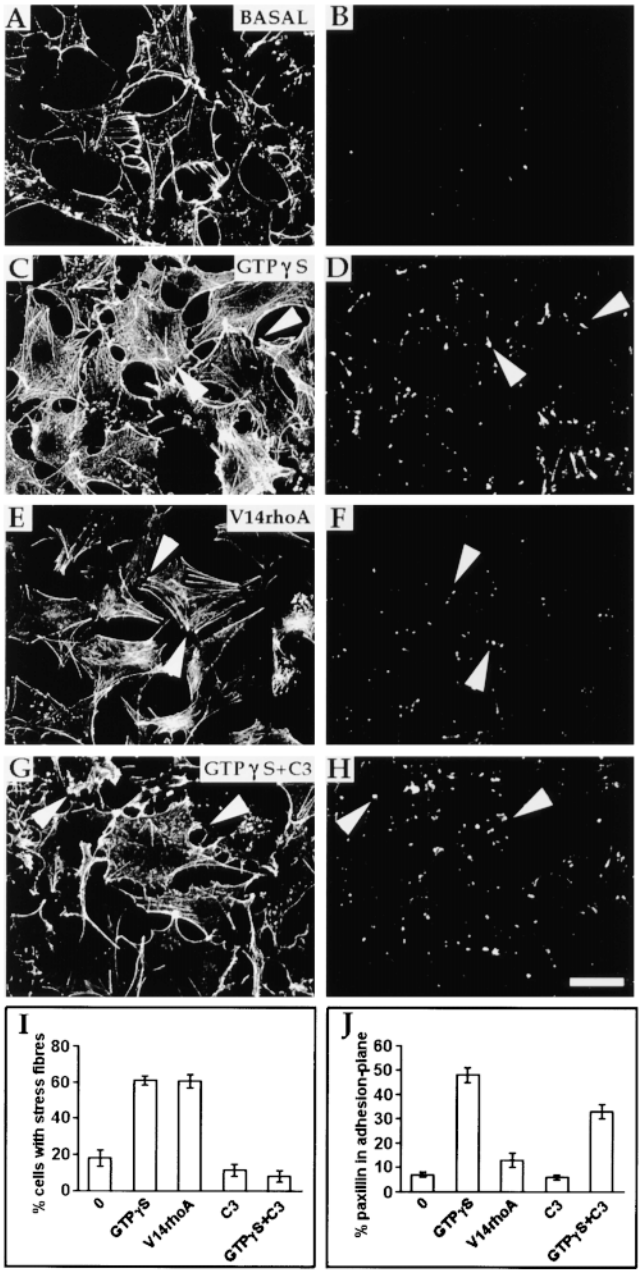

Figure 3. The GTPγS-induced formation of actin stress fibers in SL-O–permeabilized cells is rho-dependent, whereas the recruitment of paxillin to focal adhesion–like structures is not. Serum-starved Swiss 3T3 cells were incubated with SL-O on ice for 10 min, and then permeabilized by incubation at 37°C for 8 min in the presence of 1 mM GDP. After this, 1 mM Mg ATP was added in the absence (*A* and *B*; *BASAL*) or presence of 50 μM GTPγS (*C*, *D*, *G*, and *H*) or 50 μg/ml GTP-loaded Val14rhoA (*E* and *F*) for 8 min. In panels *G* and *H*, the cells were pre-incubated with 0.2 μg/ml C3-transferase / 0.5 mM NAD^+ during the permeabilization period and before addition of GTPγS. F-actin was visualized with FITC-phalloidin (*A*, *C*, *E*, and *G*), and cells double stained for paxillin (*B*, *D*, *F*, and *H*) using a Texas red–labeled secondary antibody as described in Materials and Methods. FITC-phalloidin staining is presented as an extended focus image, whereas paxillin staining is presented as an optical section corresponding to the plane of adhesion. Arrowheads are in equivalent positions in the image pairs. Cells were then scored for the presence of actin stress fibers (*I*), and the percentage of total cellular paxillin found in the plane of adhesion (*J*) was determined as in Fig. 2 by quantitation of confocal images. Data represents the mean of five independent experiments (± SEM). Bar, 40 μm.

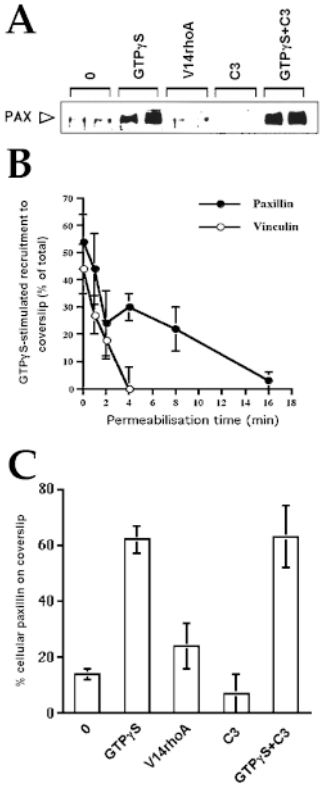

Figure 4. Analysis of paxillin content of SAM by Western blotting. (*A*) Serum-starved Swiss 3T3 cells were permeabilized with SL-O for 8 min in the presence of 1 mM GDP at 37°C. After this, 1 mM Mg ATP was added in the absence (*0*) or presence of 50 μM GTPγS or 50 μg/ml GTP-loaded Val14rhoA for 8 min. In some cases, 0.2 μg/ml C3-transferase was included with 0.5 mM NAD^+ during the permeabilization period, and before addition of GTPγS. The paxillin content of SAM from duplicate coverslips was then determined by Western blotting. (*B*) Cells were permeabilized for various times and then challenged with 1 mM Mg ATP in the absence or presence of GTPγS (as in Fig. 2, *C* and *D*). SAM was then prepared by wet cleavage at 4°C. The vinculin (○) and paxillin (●) contents of SAM were determined by Western blotting and a quantitative estimate of these obtained by densitometric scanning of the blots. The basal values (ATP alone) were then subtracted from those found in the presence of GTPγS (ATP + GTPγS) and plotted as GTPγS-stimulated recruitment. These data represent the mean (± SEM) of values obtained from three separate experiments. (*C*) Quantitative analysis of the paxillin content of SAM from experiments such as that displayed in *A*. These data represent the mean (± SEM) of values obtained from six separate experiments.

to the Golgi apparatus (Mazaki et al., 1998). Paxillin staining in the perinuclear region of serum-starved cells appears particulate in nature, and the possibility that paxillin redistribution into focal adhesions might involve vesicular transport, a process regulated by proteins such as the small GTP-binding protein ARF1, was therefore considered. The constitutively active mutant of ARF1 (Q71LARF1) was added to SL-O–permeabilized, serum-starved cells and paxillin staining and actin stress fiber assembly examined using confocal microscopy. Q71LARF1 caused the redistribution of paxillin into the plane of adhesion where it was localized in focal adhesion–like structures (Fig. 5 *F*), but it did not drive the assembly of actin stress fibers (Fig. 5 *E*). The paxillin was localized at the ends of actin filaments under the plasma membrane, a distribution that is very similar to that seen when cells in which Rho has been inactivated with C3-transferase, are treated with GTPγS (Fig. 3, *G* and *H*).

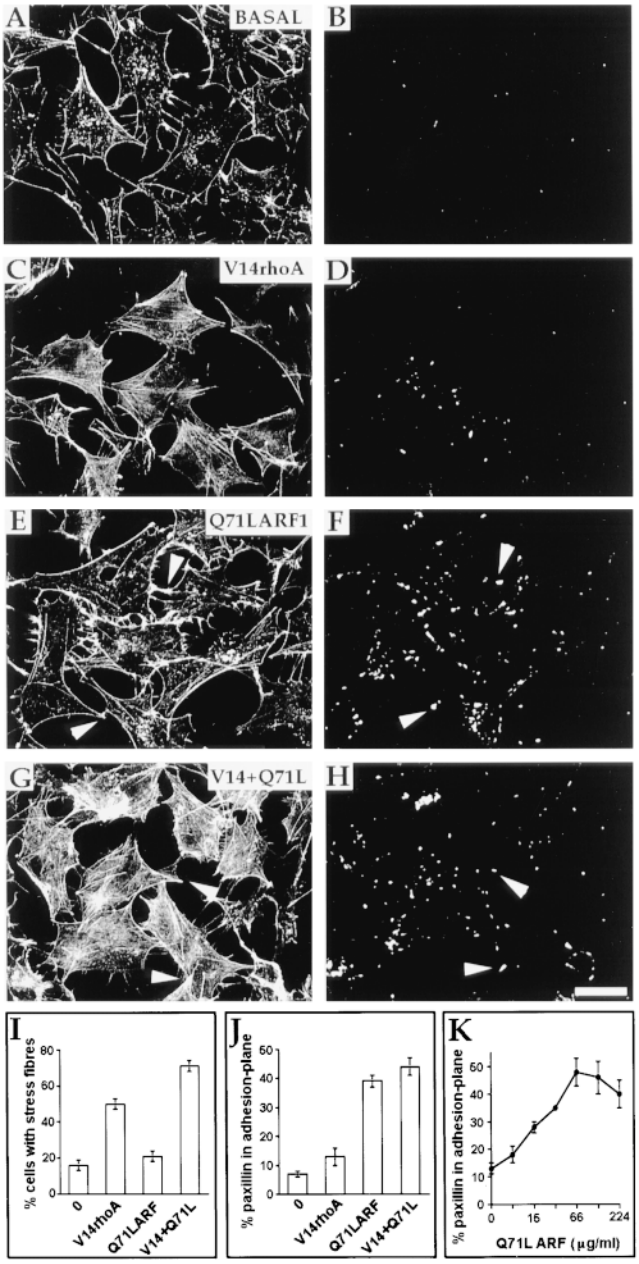

Figure 5. Q71LARF1 drives the redistribution of paxillin into focal adhesion–like structures. Serum-starved Swiss 3T3 cells permeabilized with SL-O for 8 min were treated with 1 mM Mg ATP in the absence (*A* and *B*; *BASAL*) or presence of 50 μg/ml GTP-loaded Val14rhoA (*C* and *D*), 100 μg/ml Q71LARF1 (*E* and *F*) or V14rhoA and Q71LARF1 (*G* and *H*) for 8 min. F-actin was visualized with FITC-phalloidin (*A*, *C*, *E*, and *G*) and cells double stained for paxillin (*B*, *D*, *F*, and *H*) using a Texas red–labeled secondary antibody. FITC-phalloidin staining is presented as an extended focus image, whereas paxillin staining is presented as an optical section corresponding to the plane of adhesion. Arrowheads are in equivalent positions on the image pairs. Cells were scored for the presence of actin stress fibers (*I*) and the percentage of total cellular paxillin found in the plane of adhesion was determined as for Fig. 2 by quantitation of confocal images (*J*). Data represents the mean of four independent experiments (± SEM). A dose-response curve of the Q71LARF1-induced recruitment of paxillin into the plane of adhesion is presented as the mean (± SEM) of three separate experiments (*K*). Bar, 40 μm.

Quantitative analysis of the confocal images showed that Q71LARF1 produced a 5.6-fold increase in paxillin staining in the plane of adhesion whereas V14RhoA produced only a twofold increase (Fig. 5 *J*). In contrast, V14RhoA produced a large increase in the number of cells with actin stress fibers whereas Q71LARF1 had no significant effect in this regard (Fig. 5 *I*). Interestingly, the addition of Q71LARF1 and V14RhoA together caused a significant increase in the number of cells with actin stress fibers (Fig. 5 *I*) and an apparent increase in the intensity of FITC-phalloidin staining (Fig. 5 *G*), when compared with the effect of V14RhoA alone (Fig. 5 *C*). Q71LARF1 and V14RhoA together had a lesser effect on the level of paxillin staining in the plane of adhesion, although the paxillin-containing focal adhesions were somewhat more discrete (Fig. 5 *H*) than when Q71LARF1 was added alone (Fig. 5 *F*). Investigation of the dose response curve for Q71LARF1 showed that it produced a half-maximal response at ~20 μg/ml (Fig. 5 *K*) that is in the low micromolar range.

The effect of ARF1 on the amount of paxillin associated with SAM was also examined by wet cleavage. The Q71LARF1 mutant caused a 4.2-fold increase in paxillin in SAM, but the effect was somewhat variable as indicated by the large standard errors (Fig. 6). Although V14RhoA

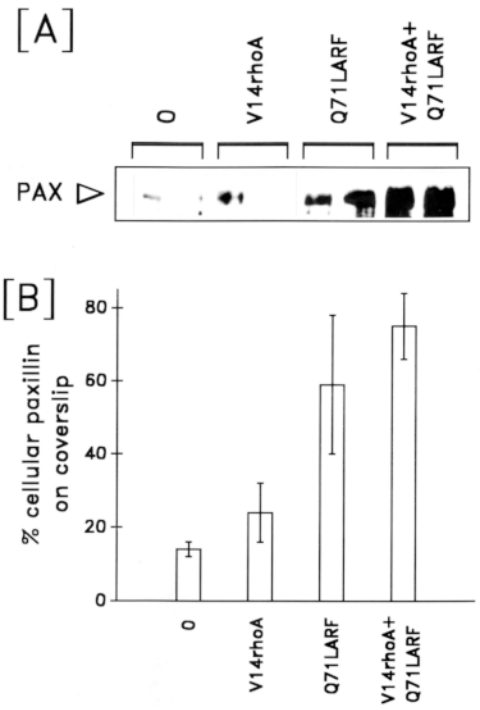

Figure 6. Q71LARF1 increases the paxillin content of SAM. (*A*) Serum-starved Swiss 3T3 cells permeabilized for 8 min with SL-O were treated with 1 mM Mg ATP (*0*) in the presence of 50 μg/ml GTP-loaded Val14rhoA, 100 μg/ml Q71LARF1, or V14rhoA and Q71LARF1 for 8 min. SAM was then prepared by wet cleavage at 4°C. The paxillin content of SAM from duplicate coverslips was determined by Western blotting. (*B*) Quantitative analysis of the paxillin content of SAM was obtained as for Fig. 4. The data represent the mean (± SEM) of values obtained from four separate experiments.

produced only a twofold increase at best, it did increase the response to Q71LARF1 and reduce the variable nature of the response. Overall, the results suggest that ARF1 regulates the delivery of paxillin to focal adhesions whereas Rho controls actin stress fiber formation. However, the effects of the two GTP-binding proteins would appear to be complimentary with ARF1 potentiating the effects of RhoA and vice versa.

Leakage of ARF Proteins from SL-O–permeabilized Cells Leads to Loss of GTPγS-induced Paxillin Redistribution to Focal Adhesions

A study of the rates at which ARF proteins and paxillin leak out of SL-O–permeabilized cells shows that >80% of ARF proteins have been lost within 16 min, whereas >70% of paxillin is retained (Fig. 7 *A*). The leakage of ARF is coincident with a significant reduction in the GTPγS-induced redistribution of paxillin into SAM as judged by wet cleavage and Western blotting (Fig. 7, *B* and *C*). The re-addition of wild-type ARF1 resulted in a complete restoration of the ability of GTPγS to induce paxillin redistribution into SAM. Similarly, the ability of GTPγS to induce the recruitment of paxillin into focal adhesion–like structures (as judged by confocal microscopy) was markedly reduced in cells that had been left for 16 min after SL-O permeabilization (Fig 8, *A* and *B*). Re-addition of ARF1 (Fig. 8 *C*), but not the NH_2-terminal deletion mutant of ARF1 (Δ17ARF1) (Fig. 8 *D*), restored the ability of GTPγS to induce recruitment of paxillin to these structures. Quantitative analysis showed the re-addition of ARF1 produced a threefold increase in the GTPγS-induced recruitment of paxillin to the plane of adhesion (Fig. 8 *E*). These results provide strong support to the conclusion that ARF1 regulates the distribution of paxillin between a perinuclear compartment and focal adhesions.

Δ17ARF1 Inhibits the GTPγS-stimulated Recruitment of Paxillin into Focal Adhesion–like Structures and SAM

To explore the possibility that the Δ17ARF1 mutant might act as a dominant-negative mutant, the effect of Δ17ARF1 on the GTPγS-stimulated recruitment of paxillin into focal adhesions was investigated. The results showed that the GTPγS-stimulated recruitment of paxillin into focal adhesion–like structures at the ends of actin filaments (Fig. 9, *A* and *B*) was almost completely blocked by Δ17ARF1 (Fig. 9, *C* and *D*). Quantitative analysis of confocal microscope images confirmed this finding (Fig. 9 *F*). Similarly, the Δ17ARF1 mutant markedly inhibited the ability of GTPγS to stimulate the recruitment of paxillin into SAM as judged by quantitative analysis of Western blots (Fig. 10, *A* and *B*). However, Δ17ARF1 did not appear to affect the formation of actin stress fibers (Fig. 9, *C* and *E*), although they were finer and stained less intensely with FITC-phalloidin than those produced in response to GTPγS alone (Fig. 9, *A* and *C*). Analysis of the dose-inhibition curve for Δ17ARF1 showed that it produced half-maximal inhibition of paxillin recruitment to the plane of adhesion at ~20 μg/ml (Fig. 9 *G*), which is very similar to the concentration of Q71LARF1 required to stimulate paxillin recruitment (Fig. 5 *K*).

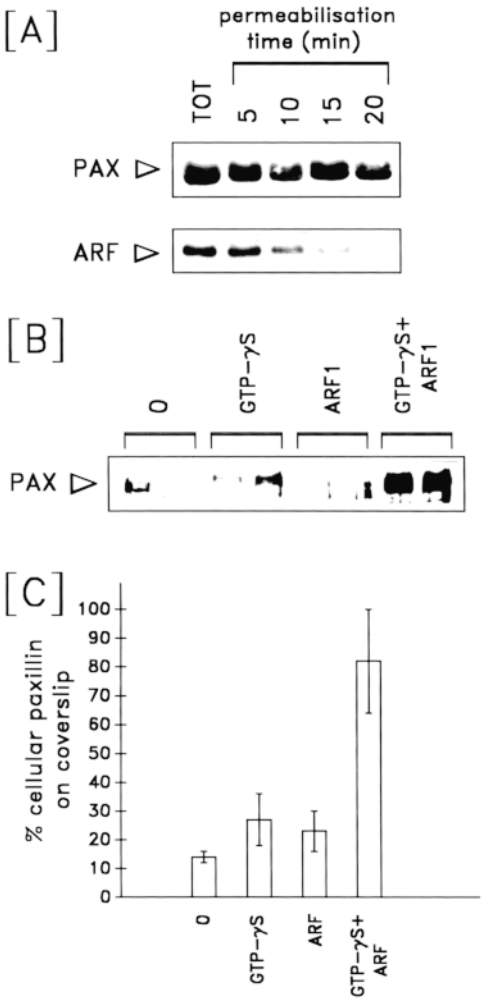

Figure 7. Loss of GTPγS-induced paxillin redistribution into SAM after ARF leakage, and reconstitution by ARF1 addition. (*A*) Serum-starved Swiss 3T3 cells were incubated with SL-O on ice for 10 min and permeabilized by incubation at 37°C in the presence of 1 mM GDP. The paxillin and ARF remaining in the cell monolayer was determined by Western blotting at various times after permeabilization. (*B*) Cells were permeabilized for 16 min in the presence of 1 mM GDP. After this, 1 mM MgATP was added for 8 min in the absence (*0*) or presence of 50 μM GTPγS, with or without the addition of 100 μg/ml ARF1. SAM was then prepared by wet cleavage at 4°C, and the paxillin content of SAM from duplicate coverslips was determined by Western blotting. (*C*) Quantitative analysis of the paxillin content of SAM was obtained as for Fig. 4. These data represent the mean (± SEM) of values obtained from four separate experiments.

Microinjection of ARF Proteins into Serum-starved Swiss 3T3 Cells Regulates Paxillin Recruitment to Focal Adhesion–like Structures

To investigate whether the effects of ARF1 on paxillin localization could be demonstrated in intact cells, Q71LARF1 was microinjected into serum-starved Swiss 3T3 cells, and

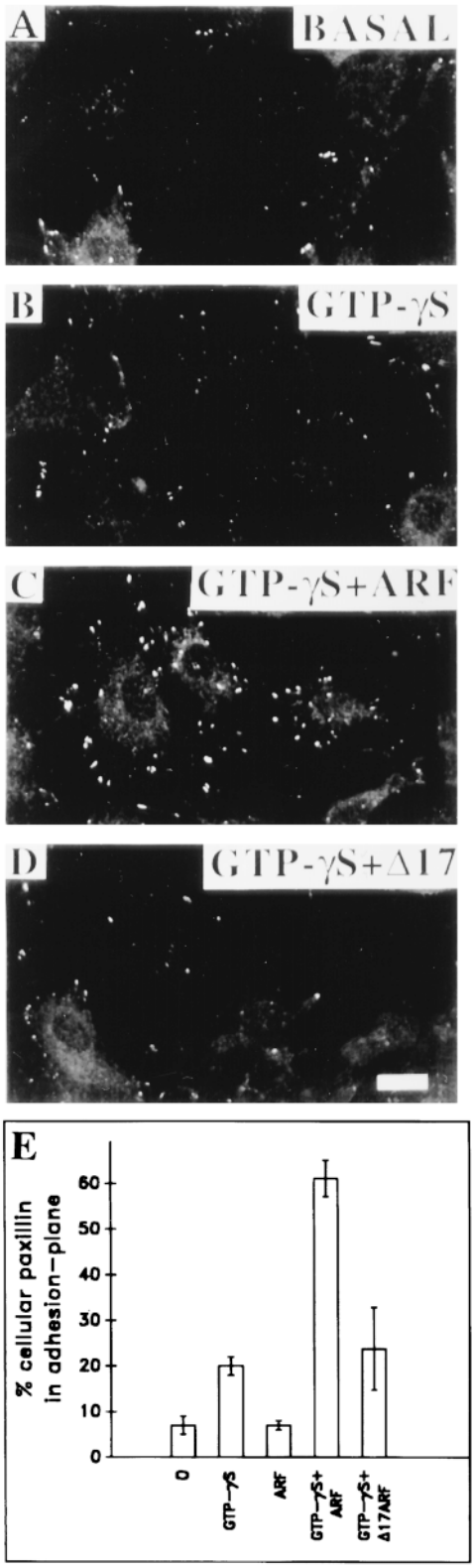

Figure 8. Loss of GTPγS-induced paxillin redistribution into the adhesion plane after ARF leakage; reconstitution by ARF1 addition. Cells were permeabilized for 16 min in the presence of 1 mM GDP. After this 1 mM MgATP was added in the absence (*A*; *BASAL*) or presence of 50 μM GTPγS (*B–D*) for 8 min. 100 μg/ml ARF1 (*C*) or Δ17ARF1 (*D*; GTPγS+Δ17) was included with the GTPγS challenge. Paxillin was visualized by indirect immunofluorescence and its distribution analyzed by confocal microscopy. An optical plane centered 0.5 μm above the surface of the coverslip (adhesion-plane) is presented. (*E*) The fluorescence intensity from the adhesion plane was expressed as a percentage of the total cellular fluorescence as for Fig. 2. These data represent the mean (± SEM) of values obtained from 4 separate experiments. Bar, 20 μm.

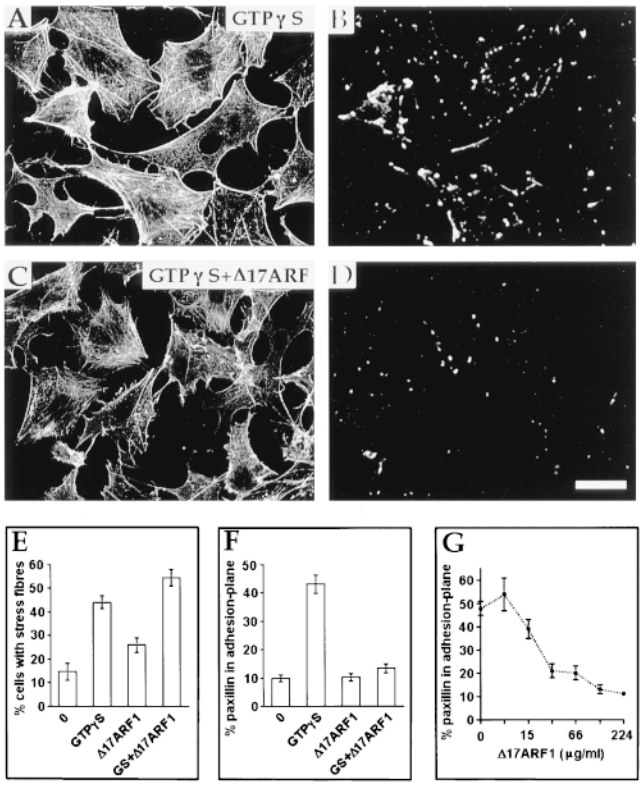

Figure 9. Δ17ARF1 inhibits the ability of GTPγS to recruit paxillin to focal adhesions. Serum-starved Swiss 3T3 cells were incubated with SL-O on ice for 10 min and permeabilized by incubation at 37°C for 8 min in the presence of 1 mM GDP without (*A* and *B*) and with (*C* and *D*) 100 μg/ml Δ17ARF1. After this, 1 mM Mg ATP and 50 μM GTPγS were added in the continued absence (*A* and *B*) or presence of (*C* and *D*) of Δ17ARF1. FITC-phalloidin staining (*A* and *C*) is presented as an extended focus image, whereas paxillin staining (*B* and *D*) is presented as an optical section corresponding to the plane of adhesion. Cells were then scored for the presence of actin stress fibres (*E*) and the percentage of total cellular paxillin found in the plane of adhesion was determined (*F*). Data represents the mean of four independent experiments (± SEM). A dose inhibition curve showing the ability of Δ17ARF1 to oppose the GTPγS-induced recruitment of paxillin to the plane of adhesion is presented as the mean (± SEM) of three separate experiments (*G*). Bar, 40 μm.

the cells stained 10 min later for paxillin (Fig. 11, *A*, *C*, *E*, and *G*) or F-actin (Fig. 11, *B*, *D*, *F*, and *H*). Microinjection of Q71LARF1 lead to the appearance of paxillin in large focal adhesion–like structures (Fig. 11 *C*) whereas microinjection of buffer alone had no such effect (Fig. 11 *A*). The response to V14RhoA was much less pronounced (Fig. 11 *E*), but when Q71LARF1 and V14RhoA were microinjected together, the cells assembled numerous large

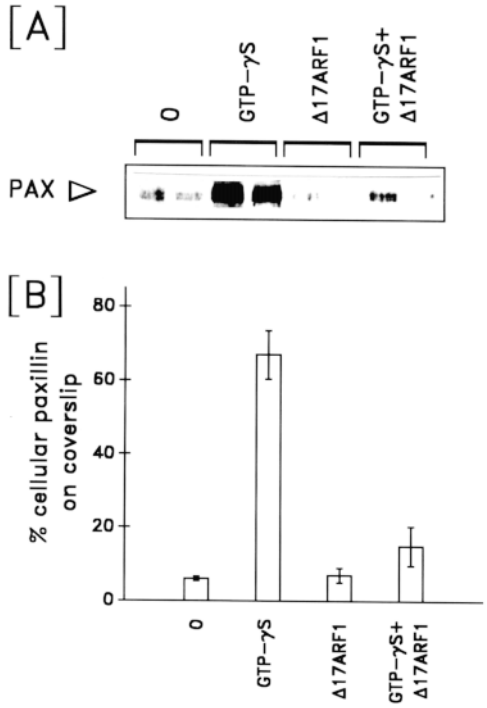

Figure 10. Δ17ARF1 inhibits the ability of GTPγS to increase the paxillin content of SAM. Serum-starved Swiss 3T3 cells were incubated with SL-O on ice for 10 min, and permeabilized by incubation at 37°C for 8 min in the presence of 1 mM GDP, without and with 100 μg/ml Δ17ARF1. After this, permeabilized cells were treated with 1 mM Mg ATP for 8 min with or without 50 μM GTPγS in the continued absence or presence of Δ17ARF1. SAM was then prepared by wet cleavage at 4°C, and the paxillin content of SAM from duplicate coverslips was determined by Western blotting. (*B*) Quantitative analysis of the paxillin content of SAM was obtained as for Fig. 4. These data represent the mean (± SEM) of values obtained from four separate experiments.

paxillin-containing focal adhesion–like structures (Fig. 11 *G*). Q71LARF1 did not stimulate the assembly of actin stress fibers although it lead to the marked accumulation of F-actin at highly localized sites just under the plasma membrane (Fig. 11 *D*). As expected V14RhoA stimulated stress fiber formation (Fig. 11 *F*). However, Q71LARF1 markedly potentiated the effect of V14RhoA on the assembly of actin stress fibers, and these stained much more intensely with FITC-phalloidin (Fig. 11 *H*) than those produced in response to V14RhoA alone (Fig. 11 *F*), reinforcing the idea that ARF1 might contribute to the regulation of the actin cytoarchitecture.

The effects of microinjecting Δ17ARF1 into serum-starved Swiss 3T3 cells on the LPA-induced assembly of actin stress fibers and paxillin-containing focal adhesion was also examined. Whereas cells microinjected with buffer alone assembled numerous paxillin-containing focal adhesions in response to LPA (Fig. 12 *A*), this response was almost completely blocked in cells microinjected with Δ17ARF1, although uninjected neighboring cells showed strong staining for paxillin in focal adhesions (Fig. 12, *C* and *E*). Microinjection of Δ17ARF1 did not block LPA-induced actin stress fiber assembly, although the stress fibers formed stained much less intensely for F-actin (Fig. 12, *D* and *F*) than those seen in uninjected neighboring cells or cells injected with buffer alone (Fig. 12 *B*). The results obtained using Q71LARF1 and Δ17ARF1 in microinjection studies are very similar to those obtained using permeabilized cells, and provide strong evidence that ARF1 plays a role in the recruitment of paxillin to focal adhesion–like structures.

Discussion

We have used serum-starved Swiss 3T3 cells permeabilized with SL-O to investigate the relationship between the assembly of actin stress fibers and the recruitment of vinculin and paxillin to focal adhesions. Whereas addition of GTPγS at the time of permeabilization stimulated the recruitment of vinculin and paxillin from a perinuclear location to focal adhesion–like structures at the ends of actin stress fibers, this coordinated response was lost with time. Thus, when GTPγS was added 8 min after permeabilization, paxillin but not vinculin was recruited to the ends of actin stress fibers. GTPγS also stimulated the recruitment of paxillin and vinculin into SAM, and again the vinculin response decayed much more rapidly than that for paxillin. These results suggest that paxillin and vinculin targeting to focal adhesions are regulated by different mechanisms. Experiments with C3 transferase showed that the GTPγS-stimulated recruitment of paxillin into focal adhesion–like structures was largely independent of Rho, although Rho was required for the assembly of actin stress fibers. However, the small GTP-binding protein ARF1 (Q71LARF1) was able to support the GTPγS-stimulated recruitment of paxillin into focal adhesion–like structures and SAM, without promoting actin stress fiber assembly. Moreover, the Δ17ARF1 mutant blocked these effects. The role of ARF1 in regulating paxillin recruitment to focal adhesion–like structures was confirmed by microinjection of Q71LARF1 into serum-starved cells, and by the demonstration that microinjection of Δ17ARF1 blocked the LPA-induced recruitment of paxillin to focal adhesions. Interestingly, the V14RhoA-induced assembly of actin stress fibers was potentiated by Q71LARF1. These results suggest that these two small GTP-binding proteins activate complimentary pathways that together lead to the formation of paxillin-rich focal adhesions at the ends of prominent actin stress fibers.

Mechanism of Rho Action

The mechanisms by which Rho exerts its effects on the assembly of actin stress fibers and focal adhesions are slowly being elucidated (Machesky and Hall, 1996; Ridley, 1996; Burridge et al., 1997). Rho has been shown to activate an S/T kinase (Leung et al., 1995; Amano et al., 1996) which phosphorylates myosin light chain phosphatase leading to its inactivation (Kimura et al., 1996). Rho kinase has also been shown to phosphorylate myosin light chain directly (Amano et al., 1996). Both pathways are likely to contribute to increased myosin light chain phosphorylation, which is known to result in activation of the myosin ATPase and the assembly of bipolar myosin filaments (Bur-

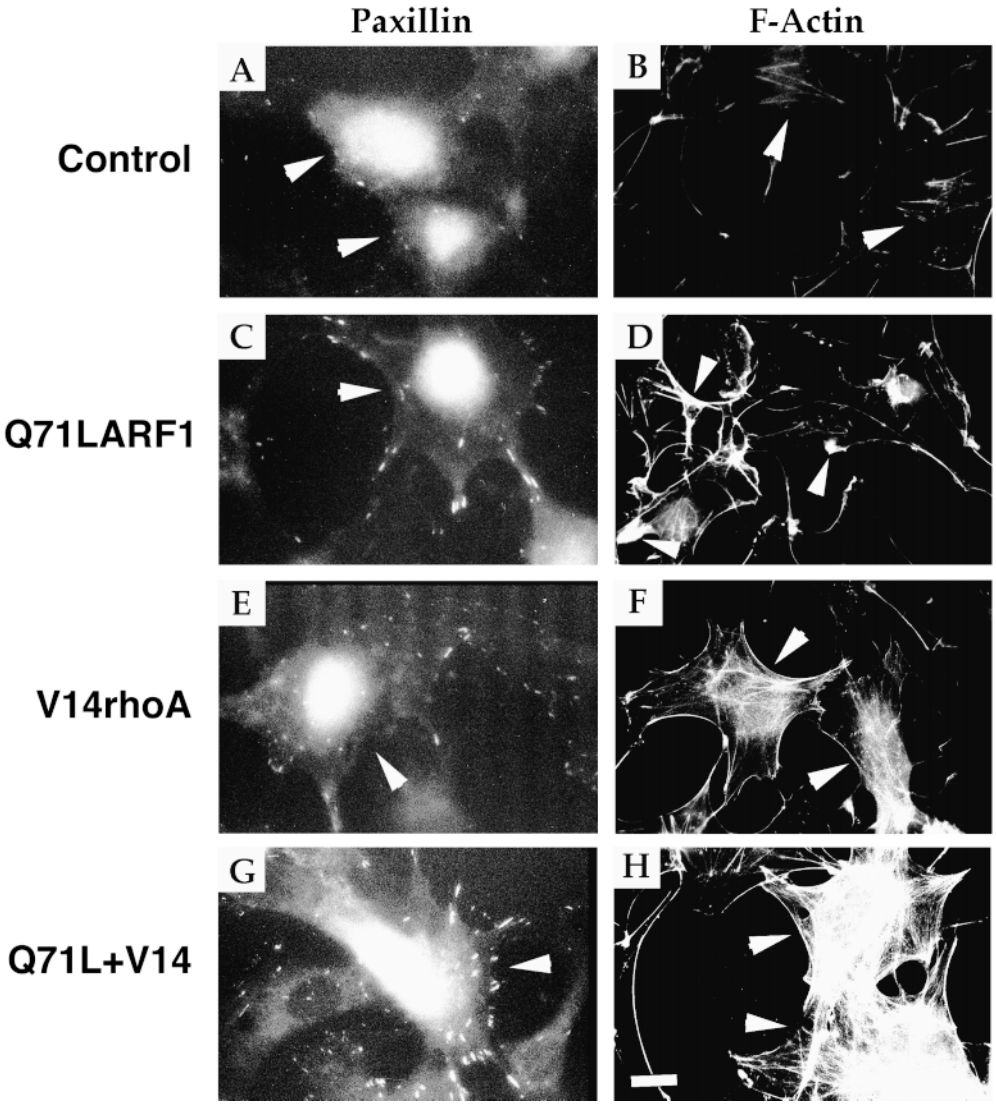

Figure 11. Microinjection of Q71LARF1 into serum-starved cells induces the formation of paxillin-containing focal adhesion-like structures. Serum-starved Swiss 3T3 cells were microinjected with buffer alone (*A* and *B*), Q71LARF1 (*C* and *D*), V14rhoA (*E* and *F*) or Q71LARF1 plus V14rhoA (*G* and *H*). Needle concentrations of proteins were 500 μg/ml. TRITC-Dextran was included in the microinjection buffer to identify injected cells. Cells were fixed 10 min after injection and stained for either paxillin (*A*, *C*, *E*, and *G*) or F-actin (*B*, *D*, *F*, and *H*). Microinjected cells are indicated by arrowheads. Staining of the nucleus and cell body in the paxillin channel is bleed-through from the TRITC-Dextran, and aids identification of microinjected cells. Bar, 10 μm.

ridge and Chrzanowska-Wodnicka, 1996). Studies with myosin light chain kinase inhibitors and the myosin ATPase inhibitor 2,3 butanedione monoxime are consistent with a hypothesis in which the tension exerted by the actomyosin contractile apparatus in adherent cells results in the alignment of actin filaments into stress fibers (Chrzanowska-Wodnicka and Burridge, 1996). Indeed, recent data suggest that Rho-induced stress fiber formation involves little new actin polymerization (Machesky and Hall, 1997) and is due largely to rearrangement of actin filaments. The signaling pathways required for Rho-dependent actomyosin contraction have been shown to be retained in escin-permeabilized smooth muscle cells for ≤30 min after permeabilization (Noda et al., 1995), and it is likely that such pathways contribute to the appearance of actin stress fibers in response to the addition of GTPγS in the present study. Thus, the GTPγS-induced assembly of actin stress fibers in SL-O–permeabilized Swiss 3T3 cells was (*a*) completely blocked by C3-transferase, (*b*) activated by the addition of V14RhoA, and (*c*) retained ≤16 min after permeabilization.

Chrzanowska-Wodnicka and Burridge (1996) have also reported that myosin light chain kinase inhibitors and the myosin ATPase inhibitor 2,3 butanedione monoxime inhibit the formation of focal adhesions, and they have proposed that contraction of actomyosin is responsible for clustering of integrins in the plane of the membrane leading to the formation of focal adhesions (Burridge and Chrzanowska-Wodnicka, 1996). Whereas this is an attractive hypothesis, other mechanisms may also contribute to focal adhesion formation. If the process were driven solely by actomyosin contraction, it should not be possible to obtain such structures in the absence of actin stress fibers. However, Nobes and Hall (1995) have reported that V14RhoA will drive the formation of focal adhesion–like structures in the presence of concentrations of cytochalasin D that block stress fiber formation. An additional reservation about the above hypothesis is that 2,3 butanedione monoxime would also be expected to inhibit unconventional myosins. At least some of these are thought to be involved in vesicular transport (Titus, 1997), and it is becoming apparent that transport of membrane vesicles to

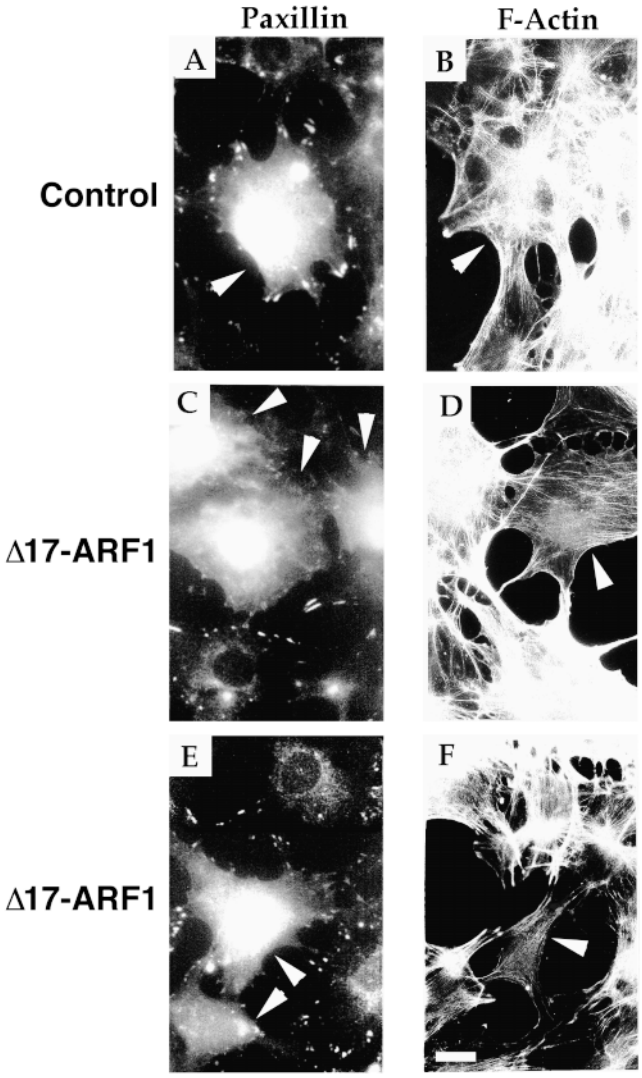

Figure 12. Microinjection of Δ17ARF1 inhibits the LPA-induced assembly of paxillin-containing focal adhesions. Serum-starved Swiss 3T3 cells were microinjected with buffer alone (*A* and *B*) or Δ17ARF1 (*C–F*) at a needle concentration of 900 μg/ml. After 20 min, the cells were stimulated with 1 μg/ml LPA for 15 min, fixed and stained for either paxillin, by indirect immunofluorescence (*A*, *C*, and *E*), or F-actin with FITC-phalloidin (*B*, *D*, and *F*). Microinjected cells are indicated by arrowheads. The nuclear and cell body staining in the paxillin channel is bleed-through from the TRITC-Dextran used to aid identification of the microinjected cells. The F-actin staining has been deliberately overexposed to show the weaker actin fibers in cells microinjected with Δ17ARF1. Bar, 10 μm.

the leading edge of cells forms part of the locomotory response (Bretscher, 1996), and may be involved in the polarized delivery of integrins to lamellipodia. Indeed, several studies have noted that disturbance of the endocytic–exocytic cycle leads to the disassembly of polarized focal adhesions (Altankov and Grinnell, 1993; Tranqui et al., 1993). It is interesting that Cdc42, which stimulates formation of filopodia and associated small focal adhesion–like structures (Nobes and Hall, 1995), is localized in the Golgi apparatus (Erickson et al., 1996), and that in *Dictyostelium discoideum*, it activates a kinase that phosphorylates the myosin I heavy chain (Lee et al., 1996).

Recruitment of Paxillin to Focal Adhesions: Role of ARF1

Immediately after permeabilization, the ability of GTPγS to recruit both vinculin and paxillin to focal adhesion–like structures decreases rapidly. This suggests that signaling components necessary for their recruitment are rapidly lost from the cells. The kinetics of this initial run-down phase are very similar for both vinculin and paxillin suggesting that there may be mechanisms for recruiting complexes containing both vinculin and paxillin (possibly bound to each other) to focal adhesions. However, the run-down kinetics of paxillin recruitment are clearly biphasic and contain a second component that runs-down more slowly (Figs. 2 *D* and 4 *B*). The ability of GTPγS to elicit this phase of paxillin recruitment to focal adhesion–like structures is only partially blocked by C3-transferase, and is only weakly stimulated by V14RhoA. This supports the conclusion that contraction of the actomyosin network is not the only mechanism involved in focal adhesion assembly, and implicates other GTP-binding proteins in this process. The results described here provide strong evidence that ARF1 regulates, at least in part, the recruitment of paxillin to focal adhesion–like structures. Thus, in SL-O–permeabilized, serum-starved Swiss 3T3 cells, Q71LARF1 caused a dramatic redistribution of paxillin from the perinuclear region to focal adhesion–like structures, and lead to a marked increase in the paxillin content of SAM. Loss of ARF proteins after permeabilization was coincident with a reduction in GTPγS-induced paxillin recruitment to focal adhesions and SAM, and the system could be resensitized by addition of wild-type ARF1. Conversely, Δ17ARF1 inhibited the GTPγS-stimulated recruitment of paxillin to focal adhesions and SAM. A role for ARF1 in regulating the localization of paxillin was confirmed in intact cells by microinjection experiments. It is interesting that even in the intact cell, microinjection of Q71LARF1 induced the assembly of paxillin-rich focal adhesions that were poor in vinculin (not shown). This indicates that paxillin recruitment can be regulated independently from that of other focal adhesion proteins. The idea that recruitment of some components of focal adhesions may be controlled independently of others is well established. For example, the incorporation of talin into focal adhesion precursors precedes that of vinculin (DePasquale and Izzard, 1991), and PDGF treatment of Balb/c 3T3 cells resulted in a more rapid loss of vinculin from focal adhesions than talin (Herman and Pledger, 1985). Studies using beads coated with integrin antibodies suggest that integrin cross-linking is sufficient to recruit tensin and $pp125^{FAK}$ to the cytoplasmic face of integrins (Miyamato et al., 1995), whereas the recruitment of other cytoskeletal proteins required both integrin aggregation and ligand occupancy.

The nature of the protein–protein interactions that target paxillin to focal adhesions has not been fully resolved. Paxillin has been reported to bind directly to β1-integrin cytoplasmic domain peptides (Schaller et al., 1995), and to the focal adhesion proteins vinculin (Wood et al., 1994)

and pp125^{FAK} (Bellis et al., 1995). However, De Nichilo and Yamada (1996) have shown that paxillin can be recruited to focal adhesions in the absence of pp125^{FAK}. Recent studies have shown that neither the pp125^{FAK} or vinculin-binding sites in paxillin are able to direct the protein to focal adhesions, and that the major determinant is contained within the LIM3 domain (Brown et al., 1996). At present, the binding partner for this domain has not been identified, but the authors suggest that LIM3 binds to NPXY motifs of β integrins, and paxillin could be a passenger on the vesicles delivering integrins to sites of adhesion.

Mechanisms of ARF1 Action in Paxillin Recruitment

ARF1 is required for coatamer assembly on Golgi transport vesicles (Serafini et al., 1991) and is known to act synergistically with Rho to activate PLD1. It is possible, therefore, that the mechanism underlying the effects of ARF1 observed in the present study could be mediated by PLD. However, this seems unlikely because Q71LARF1, which stimulates paxillin recruitment to focal-adhesion–like structures does not activate PLD in COS7 cells (Park et al., 1997), or in permeabilized HL60 cells (Jones, D.H., A. Fensome, and S. Cockcroft, submitted for publication). Moreover, Δ17ARF1, which is a potent inhibitor of paxillin recruitment both in SL-O–permeabilized and intact Swiss 3T3 cells, is unable to inhibit PLD activity in HL60 cells, although it does block recruitment of coatamer to Golgi-derived vesicles (Jones, D.H., A. Fensome, and S. Cockcroft, submitted for publication). The small GTP-binding protein, Cdc42 (Erickson et al., 1996), which drives the formation of filopodia, is colocalized with ARF1 in the Golgi apparatus. Cdc42 is able to trigger the assembly of small focal adhesion–like structures at the ends of filopodia that contain many of the same components as the larger focal adhesions found at the ends of actin stress fibers (Nobes and Hall, 1995). Whether there is any cross-talk between ARF1 and Cdc42 has not been established. However, the possibility that ARF1 and Rac signal through a common pathway is raised by the finding that Arfaptin 2, a recently identified ARF1-binding protein (Kanoh et al., 1997), is almost identical to the Rac-binding protein POR1, which has been implicated in Rac-induced membrane ruffling (Joneson et al., 1996). A role for ARF1 in the control of integrin-mediated cell adhesion is indicated by recent studies on the proteins GRP1 and cytohesin-1 that contain a domain capable of stimulating both guanine nucleotide exchange on ARF1, and the activation of β2-integrins (Kolanus et al., 1996; Klarlund et al., 1997).

Regulation of Vinculin Targeting

The ability of GTPγS to stimulate vinculin recruitment to focal adhesion–like structures in SL-O–permeabilized Swiss 3T3 cells is lost within 5 min of permeabilization. This is not because the protein itself has leaked out of the cell, and ~80% of the cytoplasmic focal adhesion proteins such as vinculin, paxillin, pp125^{FAK}, and talin are retained up to 20 min after permeabilization (data not shown). Presumably, the GTPγS-activated signaling pathways necessary for vinculin targeting to focal adhesions are compromised within 5 min of permeabilization. Using digitonin-permeabilized Swiss 3T3 cells, Mackay et al. (1997) have shown that the ability of GTPγS to stimulate recruitment of vinculin to focal adhesions, was lost over a similar time course. Interestingly, they went on to show that the addition of moesin and other members of the ERM family of proteins resensitized the digitonin-permeabilized cells to GTPγS, although the moesin did not leak out of the cell. The authors speculate that endogenous moesin becomes inactive shortly after digitonin permeabilization. ERM proteins and vinculin exhibit intramolecular interactions that are relieved by PIP2 (Niggli et al., 1995; Hirao et al., 1996), and both are consequently activated in the presence of the lipid (Gilmore and Burridge, 1996; Weekes et al., 1996; Hirao et al., 1996). It is possible therefore, that signaling pathways leading to GTPγS-induced PIP2 synthesis become inactivated shortly after permeabilization (Fensome et al., 1996).

ARF1 Potentiates the Ability of rho to Induce Actin Stress Fibers

Whereas Q71LARF1 (in the absence of rho) does not lead to stress fiber formation in either SL-O permeabilized or intact Swiss 3T3 cells, it does cause the appearance of ill-defined actin-rich structures at the cell periphery. These are particularly noticeable in microinjected cells (Fig. 11 *D*). However, Q71LARF1 does markedly potentiate the ability of rho to induce the formation of stress fibers that stain intensely for F-actin (compare Fig. 11, *F* and *H*). Conversely, microinjection of Δ17ARF1 into serum-starved Swiss 3T3 cells dramatically reduces the FITC-phalloidin staining of the LPA-induced stress fibers, although Δ17ARF1 does not seem to inhibit the formation of stress fibers per se (Fig. 12, *D* and *F*). These findings are consistent with the hypothesis that rho acts to stimulate the contraction and alignment of pre-existing actin filaments whereas ARF1 potentiates this effect by inducing actin polymerization. Based on the established role of ARF1 in the assembly of the coatomer complex on Golgi-derived vesicles (Serafini et al., 1991), it is tempting to speculate that it might also promote the assembly of a complex of proteins on a population of vesicles that are able to initiate actin polymerization after delivery to sites of substrate adhesion at the ventral plasma membrane. Interestingly, the Sec6/8 complex has recently been shown to be recruited to cell–cell contacts, and this then directs Golgi-derived transport vesicles to the baso-lateral membrane in polarized epithelial cells (Grindstaff et al., 1998).

In conclusion, this study establishes the potential of using SL-O–permeabilized serum-starved Swiss 3T3 cells to study the assembly of focal adhesions. The selective loss of cytosolic components and the inactivation of certain cellular responses has allowed us to dissociate several events that are normally coordinately regulated. Thus, we have shown that the recruitment of paxillin from a perinuclear compartment to focal adhesion–like structures is regulated by ARF1, and that this can occur independently of vinculin recruitment and the Rho-dependent assembly of actin stress fibers.

We thank A. Hall (University College London) for the V14RhoA and C3-transferase expression plasmids, and A. Ridley for helpful discussion of the manuscript.

The work in D.R. Critchley's laboratory was supported by the Medical Research Council, UK, and that in S. Cockcroft's laboratory by the Wellcome Trust.

Received for publication 22 July 1998 and in revised form 2 November 1998.

References

Altankov, G., and F. Grinnell. 1993. Depletion of intracellular potassium disrupts coated pits and reversibly inhibits cell polarization during fibroblast spreading. *J. Cell Biol.* 120:1449–1459.

Amano, M., M. Ito, K. Kimura, Y. Fukata, K. Chihara, T. Nakano, Y. Matsuura, and K. Kaibuchi. 1996. Phosphorylation and activation of myosin by Rho-associated kinase (Rho-kinase). *J. Biol. Chem*. 271:20246–20249.

Barry, S., and D.R. Critchley. 1994. The RhoA-dependent assembly of focal adhesions in Swiss 3T3 cells is associated with increased tyrosine phosphorylation and the recruitment of both $pp125^{FAK}$ and protein kinase C-δ to focal adhesions. *J. Cell Sci*. 107:2033–2045.

Barry, S.T., H.M. Flinn, M.J. Humphries, D.R. Critchley, and A.J. Ridley. 1996. Requirement for Rho in integrin signalling. *Cell Adhesion Commun*. 4:387–398.

Bellis, S.L., J.T. Miller, and C.E. Turner. 1995. Characterization of tyrosine phosphorylation of paxillin in vitro by focal adhesion kinase. *J. Cell Biol*. 118:831–839.

Brands, R., and C.A. Feltkamp. 1988. Wet cleaving of cells: a method to introduce macromolecules into the cytoplasm. *Exp. Cell Res*. 176:309–318.

Bretscher, M.S. 1996. Moving membrane up to the front of migrating cells. *Cell.* 85:465–467.

Brown, M.C., J.A. Perrota, and C.E. Turner. 1996. Identification of LIM3 as the principal determinant of paxillin focal adhesion localization and characterization of a novel motif on paxillin directing vinculin and focal adhesion kinase binding. *J. Cell Biol*. 135:1109–1123.

Burridge, K., and M. Chrzanowska-Wodnicka. 1996. Focal adhesions, contractility, and signalling. *Annu. Rev. Cell Dev. Biol*. 12:463–519.

Burridge, K., M. Chrzanowska-Wodnicka, and C. Zhong. 1997. Focal adhesion assembly. *Trends Cell Biol*. 7:342–347.

Chong, L.D., A. Traynor-Kaplan, G.M. Bokoch, and M.A. Schwartz. 1994. The small GTP-binding protein Rho regulates a phosphatidylinositol 4-phosphate 5-kinase in mammalian cells. *Cell.* 79:507–513.

Chrzanowska-Wodnicka, M., and K. Burridge. 1996. Rho-stimulated contractility drives the formation of stress fibers and focal adhesions. *J. Cell Biol*. 133: 1403–1415.

Cockcroft, S., G.M.H. Thomas, A. Fensome, B. Geny, E. Cunningham, I. Gout, I. Hiles, N.F. Totty, O. Truong, and J.J. Hsuan. 1994. Phospholipase D: a downstream effector of arf in granulocytes. *Science.* 263:523–526.

Craig, S.W., and R.P. Johnson. 1996. Assembly of focal adhesions: progress, paradigms, and portents. *Curr. Opin. Cell Biol.* 8:74–85.

Crowley, E., and A.F. Horwitz. 1995. Tyrosine phosphorylation and cytoskeletal tension regulate the release of fibroblast adhesions. *J. Cell Biol*. 131:525–537.

DeNichilo, M.O., and K.M. Yamada. 1996. Integrin α(v)β(5)-dependent serine phosphorylation of paxillin in cultured human macrophages adherent to vitronectin. *J. Biol. Chem*. 271:11016–11022.

DePasquale, J.A., and C.S. Izzard. 1991. Accumulation of talin in nodes at the edge of the lamellipodium and separate incorporation into adhesion plaques at focal contacts in fibroblasts. *J. Cell Biol*. 113:1351–1359.

Erickson, J.W., C.-J., Zhang, R.A. Kahn, T. Evans, and R.A. Cerione. 1996. Mammalian Cdc42 is a brefeldin A–sensitive component of the Golgi apparatus. *J. Biol. Chem*. 271:26850–26854.

Fensome, A., E. Cunningham, S. Proner, S.K. Tan, P. Swigart, G. Thomas, J. Hsuan, and S. Cockcroft. 1996. ARF and PITP restore GTPγS-stimulated protein secretion from cytosol-depleted HL60 cells by providing P1P2 synthesis. *Curr. Biol*. 6:730–738.

Fukami, K., N. Sawada, T. Endo, and T. Takenawa. 1996. Identification of a phosphatidylinositol 4,5-bisphosphate-binding site in chicken skeletal muscle α-actinin. *J. Biol. Chem*. 271:2646–2650.

Gilmore, A.P., and K. Burridge. 1996. Regulation of vinculin binding to talin and actin by phosphatidylinositol-4-5-bisphosphate. *Nature.* 381:531–535.

Girard, P.R., and R.M. Nerem. 1995. Shear stress modulates endothelial cell morphology and F-actin organisation through the regulation of focal adhesion proteins. *J. Cell Physiol.* 163:179–193.

Goldschmidt-Clermont, P.J., J.W. Kim, L.M. Machesky, S.R. Rhee, and T.D. Pollard. 1991. Regulation of phospholipase C-γ1 by profilin and tyrosine phosphorylation. *Science.* 251:1231–1233.

Grindstaff, K.K., C. Yeaman, N. Anandasabapathy, S.C. Hsu, E. Rodriguez-Boulan, R.H. Scheller, and W.J. Nelson. 1998. Sec6/8 complex is recruited to cell–cell contacts and specifies transport vesicle delivery to the basal-lateral membrane in epithelial cells. *Cell.* 93:731–740.

Ha, K.S., and J.H. Exton. 1993. Activation of actin polymerization by phosphatidic-acid derived from phosphatidylcholine in IIc9 fibroblasts. *J. Cell Biol*. 123:1789–1796.

Hall, A. 1994. Small GTP-binding proteins and the regulation of the actin cytoskeleton. *Annu. Rev. Cell Biol*. 10:31–54.

Hall, A., and A.J. Self. 1986. The effect of Mg^{2+} on the guanine nucleotide exchange rate of $p21^{N\text{-}ras}$. *J. Biol. Chem*. 261:10963–10965.

Herman, B., and W.J. Pledger. 1985. Platelet-derived growth factor-induced alterations in vinculin and actin distribution in Balb/c-3T3 cells. *J. Cell Biol*. 100:1031–1040.

Hirao, M., N. Sato, T. Kondo, S. Yonemura, M. Monden, T. Sasaki, Y. Takai, S. Tsukita, and S. Tsukita. 1996. Regulation mechanism of ERM (ezrin/radixin/moesin) protein/plasma membrane association—possible involvement of phosphatidylinositol turnover and rho-dependent signaling pathway. *J. Cell Biol*. 135:37–51.

Hynes, R.O. 1992. Integrins: versatility, modulation, and signalling in cell adhesion. *Cell.* 69:11–25.

Jockusch, B.M., P. Bubeck, K. Giehl, M. Kroemaker, J. Moschner, M. Rothkegel, M. Rudiger, K. Schluter, G. Stanke, and J. Winkler. 1995. The molecular architecture of focal adhesions. *Annu. Rev. Cell Dev. Biol*. 11:379–416.

Joneson, T., M. McDonough, D. Bar-Sagi, and L. Van Aelst. 1996. Rac Regulation of actin polymerization and proliferation by a pathway distinct from jun kinase. *Science*. 274:1374–1376.

Kanoh, H., B.-T. Williger, and J.H. Exton. 1997. Arfaptin 1, a putative cytosolic target protein of ADP-ribosylation factor, is recruited to Golgi membranes. *J. Biol. Chem*. 272:5421–5429.

Kimura, K., M. Ito, M. Amano, K. Hihara, Y. Fukata, M. Nakafuku, B. Yamamori, J. Feng, T. Nakano, K. Okawa, A. Iwamatsu, and K. Kaibuchi. 1996. Regulation of myosin phosphatase by Rho and Rho-associated kinase (Rho-kinase). *Science.* 273:245–248.

Klarlund, J.K., A. Guilherme, J.J. Holik, J.V. Virbasius, A. Chawala, and M.P. Czech. 1997. Signaling by phosphoinositide-3,4,5-trisphosphate through proteins containing pleckstrin and Sec7 homology domains. *Science.* 275:1927–1930.

Kolanus, W., W. Nagel, B. Schiller, L. Zeitlman, H. Stockinger, and B. Seed. 1996. Alpha-l-beta-2 integrin/LFA-1 binding to ICAM-1 induced by cytohesin-1, a cytoplasmic regulatory molecule. *Cell.* 86:233–242.

Kuribara, H., K. Tago, T. Yokozeki, T. Sasaki, Y. Takai, N. Morii, S. Narumiya, T. Katada, and Y Kanaho. 1995. Synergistic activation of rat brain phospholipase D by ADP-ribosylation factor and RhoA p21, and its inhibition by *Clostridium botulinum* C3 exoenzyme. *J. Biol. Chem*. 270:25667–25671.

Lee, S.-F., T.T. Egelhoff, A. Mahasneh, and G.P. Cote. 1996. Cloning and characterisation of a Dictyostelium myosin I heavy chain kinase activated by Cdc42 and Rac. *J. Biol. Chem*. 271:27044–27048.

Leung, T., E. Manser, L. Tan, and L. Lim. 1995. A novel serine/threonine kinase binding the Ras-related RhoA GTPase which translocates the kinase to peripheral membranes. *J. Biol. Chem.* 270:29051–29054.

Machesky, L.M., and A. Hall. 1996. Rho: a connection between membrane receptor signalling and the cytoskeleton. *Trends Cell Biol*. 6:304–310.

Machesky, L.M., and A. Hall. 1997. Role of actin polymerization and adhesion to extracellular matrix in Rac- and Rho-induced cytoskeletal reorganization. *J. Cell Biol*. 138:913–926.

Mackay, D.J.G., F. Esch, H. Furthmayr, and A. Hall. 1997. Rho- and Rac-dependent assembly of focal adhesion complexes and actin filaments in permeabilized fibroblasts: an essential role for ezrin/radixin/moesin proteins. *J. Cell Biol*. 138:927–938.

Malcolm, K.C., C.M. Elliott, and J.H. Exton. 1996. Evidence for Rho-mediated agonist stimulation of phospholipase D in Rat1 fibroblasts. Effects of *Clostridium botulinum* C3 exoenzyme. *J. Biol. Chem*. 271:13135–13139.

Matsui, T., M. Amano, T. Yamamoto, K. Chihara, M. Nakafuku, M. Ito, K. Okawa, A. Iwamatsu, and K. Kaibuchi. 1996. Rho-associated kinase, a novel serine threonine kinase, as a target for the small GTP-binding protein Rho. *EMBO (Eur. Mol. Biol. Organ.) J*. 15:2208–2216.

Mazaki, Y., H. Uchida, O. Hino, S. Hashimoto, and H. Sabe. 1998. Paxillin isoforms in mouse. *J. Biol. Chem.* 273:22435–22441.

Miyamoto, S., S.K. Akiyama, and K.M. Yamada. 1995. Synergistic roles for receptor occupancy and aggregation in integrin transmembrane function. *Science.* 267:883–885.

Niggli, V., C. Andreoli, C. Roy, and P, Mangeat. 1995. Identification of a phosphatidylinositol-4,5-bisphosphate-binding domain in the N-terminal region of ezrin. *FEBS (Fed. Eur. Biochem. Soc.) Lett.* 376:172–176.

Nobes, C.D., and A. Hall. 1995. Rho, Rac, and Cdc42 GTPases regulate the assembly of multimolecular focal complexes associated with actin stress fibres, lamellipodia and filopodia. *Cell.* 81:53–62.

Noda, M., C. Yasuda-Fukazawa, K. Moriishi, T. Kato, T. Okuda, K. Kurokawa, and Y. Takuwa. 1995. Involvement of Rho in GTPγS-induced enhancement of phosphorylation of 20 kDa myosin light chain in vascular smooth muscle cells: inhibition of phosphatase activity. *FEBS (Fed. Eur. Biochem. Soc.) Lett*. 367:246–250.

Park, S.K., J.J. Provost, C.D. Bae, W.T. Ho, and J.H. Exton. 1997. Cloning and characterization of phospholipase D from rat brain. *J. Biol. Chem*. 272: 29263–29271.

Provost, J.J., J. Fudge, S. Israelit, A.R. Siddiqi, and J.H. Exton. 1996. Tissue-specific distribution and subcellular distribution of phospholipase D in rat: evidence for distinct RhoA and ADP-ribosylation factor (ARF)-regulated isoenzymes. *Biochem. J*. 319:285–291.

Ridley, A.J. 1996. Rho: theme and variations. *Curr. Biol*. 6:1256–1264.

Ridley, A.J., and A. Hall. 1992. The small GTP-binding protein Rho regulates the assembly of focal adhesions and actin stress fibres in response to growth

factors. *Cell*. 70:389–399.
Schaller, M.D., C.A. Otey, J.D. Hildebrand, and J.T. Parsons. 1995. Focal adhesion kinase and paxillin bind to peptides mimicking β-integrin cytoplasmic domains. *J. Cell Biol*. 130:1181–1187.
Serafini, T.L., L. Orci, M. Amherdt, M. Brunner, R.A. Kahn, and J.E. Rothman. 1991. ADP-ribosylation factor is a subunit of the coat of golgi-derived COP-coated vesicles: a novel role for a GTP-binding protein. *Cell*. 67:239–253.
Siddiqui, R.A., and D. English. 1996. Phosphatidic-acid induces calcium mobilization and actin polymerization through a tyrosine kinase-dependent mechanism in neutrophils—a potential regulatory mechanism for chemotaxis. *Blood* 88:2862.
Small, J.V. 1985. Geometry of actin-membrane attachments in the smooth-muscle cell—the localizations of vinculin and α-actinin. *EMBO (Eur. Mol. Biol. Organ.) J*. 4:45–49.
Tatham, P.E.R., and B.D. Gomperts. 1990. Cell permeabilisation. *In* Peptide Hormones—A Practical Approach. K. Siddle and J.C. Hutton, editors. IRL Press, Oxford. 257–269.
Tidball, J.G., T. Ohalloran, and K. Burridge. 1986. Talin at myotendinous junctions. *J. Cell Biol*. 103:1465–1472.
Titus, M.A. 1997. Unconventional myosins: new frontiers in actin-based motors. *Trends Cell Biol*. 7:119–123.
Tranqui, L., Y. Usson, C. Marie, and M.R. Block. 1993. Adhesion of CHO cells to fibronectin is mediated by functionally and structurally distinct adhesion plaques. *J. Cell Sci*. 106:377–387.
Weekes, J., S.T. Barry, and D.R. Critchley. 1996. Acidic phospholipids inhibit the intramolecular association between the N- and C-terminal regions of vinculin, exposing actin-binding and protein kinase C phosphorylation sites. *Biochem. J*. 314:827–832.
Whatmore, J., C.P. Morgan, E. Cunningham, K.S. Collison, K.R. Willison, and S. Cockcroft. 1996. ADP-ribosylation factor 1-regulated phospholipase D activity is localised at the plasma membrane and intracellular organelles in HL60 cells. *Biochem. J*. 320:785–794.
Wood, C.K., C.E. Turner, P. Jackson, and D.R. Critchley. 1994. Characterisation of the paxillin-binding site and the C-terminal focal adhesion targeting sequence in vinculin. *J. Cell Sci*. 107:709–717.
Yu, F.X., H.Q. Sun, P.A. Janmey, and H.L. Yin. 1992. Identification of a polyphosphoinositide-binding sequence in an actin monomer-binding domain of gelsolin. *J. Biol. Chem*. 267:14616–14621.